International Journal of Mechanical, Industrial and Aerospace Sciences
ISSN: 2517-9950
Vol:6, No:9, 2012

Vapor Bubble Dynamics in Upward Subcooled Flow Boiling During Void Evolution

Rouhollah Ahmadi, Tatsuya Ueno, Tomio Okawa

***Abstract*—**Bubble generation was observed using a high-speed camera in subcooled flow boiling at low void fraction. Constant heat flux was applied on one side of an upward rectangular channel to make heated test channel. Water as a working fluid from high subcooling to near saturation temperature was injected step by step to investigate bubble behavior during void development. Experiments were performed in two different pressures condition close to 2bar and 4bar. It was observed that in high subcooling when boiling was commenced, bubble after nucleation departed its origin and slid beside heated surface. In an observation window mean release frequency of bubble $f_{b,mean}$, nucleation site N_s and mean bubble volume $V_{b,mean}$ in each step of experiments were measured to investigate wall vaporization rate. It was found that in proximity of PNVG vaporization rate was increased significantly in compare with condensation rate which remained in low value.

***Keywords*—**Subcooled flow boiling, Bubble dynamics, Void fraction, Sliding bubble.

I. Introduction

IN subcooled flow boiling, initial bubble emerges at the location of onset of nucleate boiling (ONB) where heated surface temperature exceeds from saturation temperature. Here, void fraction was not developed in the channel until another specific point of onset of significant void (OSV) or point of net vapor generation (PNVG) in downstream flow which void significantly increased. In many industrial plants that forced convective boiling are used in heating process, void fraction in subcooled flow boiling region is an important parameter which influences the inception of two-phase flow instabilities [1]. Hence, accurate prediction of the location of OSV is strongly related to avoid from initiating flow instabilities. Furthermore, it is well known that accurate prediction of the value of average axial void fraction <α> in the subcooled region strongly depends on the accuracy of prediction of OSV [2]. Due to these important affects, many researchers attempted to correlate OSV or PNVG theoretically or experimentally in subcooled boiling .

Rouhollah Ahmadi, Department of Mechanical Engineering, Osaka University 2-1, Yamadaoka, Suita-shi, Osaka 565-0871, Japan (phone: +81-6-6879-7257; e-mail: ahmadi@ihmt.mech.eng.osaka-u.ac.jp)

Tatsuya Ueno, Department of Mechanical Engineering, Osaka University 2-1, Yamadaoka, Suita-shi, Osaka 565-0871, Japan (e-mail: ueno@ihmt.mech.eng.osaka-u.ac.jp)

Tomio Okawa, Department of Mechanical Engineering, Osaka University 2-1, Yamadaoka, Suita-shi, Osaka 565-0871, Japan, and also he is with Department of Mechanical Engineering and Intelligent Systems, The University of Electro-Communications 1-5-1, Chofugaoka, Chofu-shi, Tokyo 182-8585, Japan (e-mail: okawa.tomio@uec.ac.jp)

Lee and Bankoff [3] compared available NVG correlations with several experimental data and finally they concluded that levy [4] and Saha and Zuber [5] correlation are the best ones. Although these correlations can predict PNVG very well, however so far there is no confirmed triggering mechanism that caused sharply increase of void at PNVG. In some studies, void development at PNVG was related to the bubble behavior. Bowring [6], Levy [4] and Rogers et al. [7] assumed that at PNVG bubbles are departed from the nucleation site and propelled to the bulk liquid. In fact, bubble departure was assumed as triggering mechanism of void evolution. Regard with this point of view, PNVG was obtained by applying force balance on the nucleate bubble and find conditions that bubble

On the other hand, Saha and Zuber [5] postulated their well known correlation based on experimental data. It was introduced two different NVG mechanisms: at low mass fluxes it is controlled by local thermal conditions, whiles at high mass fluxes it is hydrodynamically controlled. These two categories were distinctly divided by Peclet number (Pe); in thermal control region Pe is lower than 70,000 and in hydrodynamic control region it is more than 70,000. To interpret significant void evolution after PNVG, it was expressed that bubbles can be detached from nucleation site when Stanton number (St) exceed from 0.0065. Since in high flow rate PNVG is controlled hydrodynamically, bubbles cannot detach from heated surface before PNVG, and therefore PNVG occurs with detachment. However, in low flow rate bubbles can detach from surface immediately after creation and move close to the heated surface and void should wait for specific thermal condition to rise up. Therefore, here it is seen that NVG is related to bubble behavior with depending to mass flux or Pe.

Recently, G. R. Warrier & V. K. Dhir [9] expressed that between ONB and OSV bubbles are small enough and are attached to heated surface. In slightly downstream from ONB bubbles can depart their origin and grow up and then lift off from the wall. At that moment void fraction can increase rapidly. It was hence concluded that the location where bubbles lift off from heated surface coincides with PNVG.

In spite of above beliefs, several experimental studies reported different bubble behavior in subcooled boiling [10]–[12], [14]. It was expressed that bubble can depart its nucleation cavity even at the location of ONB. In some cases bubbles are moved near heated surface and in some conditions bubble lifted off from wall, after departure. Therefore, it seems that NVG mechanism based on bubble behavior should be recognized considering in real state.

In the current study, void evolution in subcooled flow

boiling under moderate-pressure condition was investigated experimentally. This investigation proposed the new mechanism of NVG via image processing technique of bubble dynamics.

II. Experimental Description

A. Experimental Apparatus

A test facility was designed to investigate bubble behavior visually in subcooled flow boiling. Main experimental apparatus are depicted in the schematic diagram in Fig. 1a. Degassed, filtrated and deionized tap water was injected in the vacuumed loop, prior to the experiment. With adjustment of opening valve and electric power of canned motor pump the mass flow rate was set at desired values. The inlet liquid subcooling was adjusted using two 5 kW sheath heaters. It should be noted that a small part of liquid was delivered to a bypass line to control the system pressure by generation steam-water two-phase flow inside of it. After the steam-water mixture entered the separator through an outlet collector header, vapor phase was then sent to a condenser. The heat transfer rate in the condenser was also controlled to maintain the system pressure at desired values. The fluid temperature was reduced to a subcooling state at the cooling section before returning to the circulation pump. Temperatures and pressures were measured using K-type thermocouples and pressure transducers at the locations shown schematically in Fig. 1.

Fig. 1b depicted schematic diagram of the test section. A copper block containing two 1.2 kW cartridge heaters was covered by stainless steel jacket to construct the flow channel. The flow area was rectangular in shape of 10 mm □ 20 mm. The copper block was heated one side of the channel in 10 mm width and 400 mm length. The present heated surface was rather hydrophilic due to oxidization and its mean contact angle was measured 18º. The test section had two measuring sections at 100 and 300 mm from the bottom of the heated section. At each measuring section, the wall superheat temperature, the fluid temperature and the void fraction could be measured using thermocouple and an optical void probe, respectively. In addition, two sets of glass windows were mounted at the measuring sections for visual observation of bubbles using a high-speed camera. For the visualization, bubbles were backlight using a metal halide lamp. The visualization areas of the high-speed camera were set about 10 mm × 15 mm and 10 mm × 10 mm for 2 bar and 4 bar, respectively. The frame rate and the shutter speed were set to 6000 fps and 0.167 ms, respectively. More detail of test facility was explained in [10].

B. Experimental Condition and Parameter Measurement

In the present experiments, measurements were performed at the upper measuring section. The main experimental parameters were the pressure, the liquid subcooling, the mass flux and the heat flux. The test section pressure P was calculated from the pressures measured at the inlet and outlet

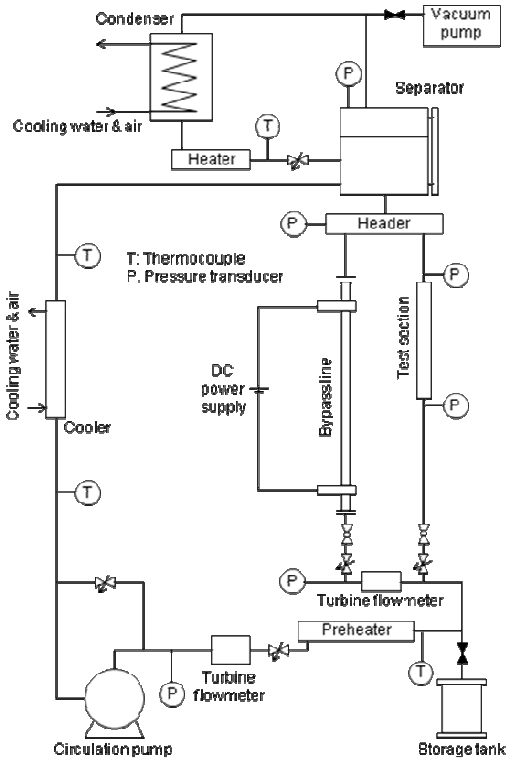

(a)

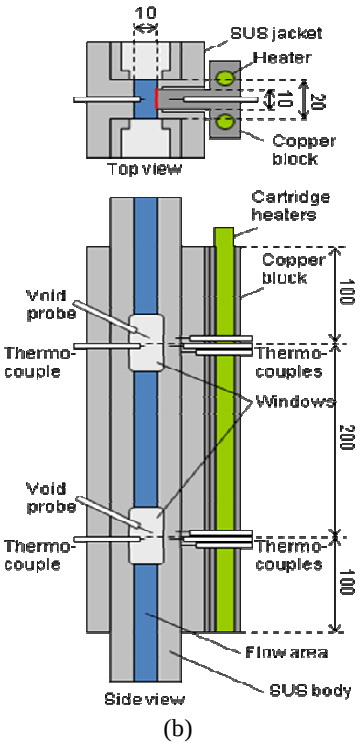

(b)

Fig. 1 Schematic diagram of the experimental facility; (a) experimental loop and (b) test section

The liquid subcooling ΔT_{sub} was determined from the liquid temperature at the outlet of the preheater and the heat applied in the test section. A turbine flow meter accurate to within ±120 mLPM was mounted after preheater to measure the total mass flow rate. The flow rate in the bypass line was measured using another turbine flow meter accurate to within ±7.5 mLPM. The measurement accuracies of P, ΔT_{sub} and G were estimated less than 10kPa, 2 K and 10 kg/m^{2}s, respectively. Two sets of experiment around 400 kg/m^{2}s mass flux and with different pressure 200 kPa and 400 kPa led current study. Main experimental conditions are summarized in Tables I and II and will be called in this paper as Exp. I and II, respectively. In each set of experiment all the fluid parameters were kept near constant value except subcooled temperature. Each set of experiment was started with single phase flow by setting wall heat flux q_w corresponding with high liquid subcooling temperature ΔT_{sub}. In order to detect the ONB condition, ΔT_{sub} was decreased slightly step by step until the first bubbles were observed in the observation window. Decreasing of ΔT_{sub} or increasing of inlet liquid temperature was continued to near saturation condition corresponding to system pressure. In each step of experiment, experimental data were acquired when system was at steady sate condition. In a stable condition bubble behavior was also recorded using the high-speed camera. In addition, the local void fraction was measured by traversing optical void probe in close to heated surface toward channel center. More detail of void measurement method is explained in the following section. Throughout the experiments, a data acquisition system attached to a personal computer recorded the temperatures, pressures, mass fluxes and heat power every 1 second.

TABLE I
MAIN EXPERIMENTAL CONDITION FOR EXP. I

Run	P (kPa)	G (kg/m^{2}s)	q_w (kW/m^2)	ΔT_{sub} (K)	ΔT_w (K)	x_{eq}	<α>
101	200	393	198	18.5	4.7	-0.0328	0.00000
102	200	395	196	16.7	6.3	-0.0295	0.00000
103	203	394	192	16.0	6.4	-0.0280	0.00000
104 (ONB)	200	394	192	14.8	7.4	-0.0256	0.00000
105	200	395	191	13. 6	8.2	-0.0233	0.00007
106	200	397	193	12.5	9.1	-0.0214	0.00031
107	201	396	196	11.7	9.3	-0.0197	0.00103
108 (NVG)	202	397	198	10.9	9.7	-0.0182	0.00162
109	202	399	195	9.8	9.8	-0.0161	0.00293
110	200	403	200	7.5	10.5	-0.0117	0.00769
111	200	403	199	5.4	10.8	-0.0077	0.01070
112	203	406	202	3.8	11.1	-0.0046	0.02277

TABLE II
MAIN EXPERIMENTAL CONDITION FOR EXP. II

Run	P (kPa)	G (kg/m^{2}s)	q_w (kW/m^2)	ΔT_{sub} (K)	ΔT_w (K)	x_{eq}	<α>
201	395	402	232	17.0	4.6	-0.0341	0.00000
202	402	401	232	16.7	5.1	-0.0335	0.00000
203	400	400	233	15.6	6.2	-0.0314	0.00000
204 (ONB)	399	400	237	14.7	7.5	-0.0296	0.00000
205	398	398	235	13.9	8.2	-0.0279	0.00000
206	400	398	198	12.9	8.7	-0.0259	0.00012
207 (NVG)	402	395	232	11.8	9.0	-0.0237	0.00018
208	401	391	228	10.7	9.2	-0.0216	0.00069
209	400	391	238	9.4	9.9	-0.0188	0.00145
210	400	386	241	8.9	10.1	-0.0180	0.00317
211	401	380	239	7.9	10.1	-0.0160	0.00427
212	402	382	243	5.9	10.4	-0.0119	0.01292
213	399	387	243	3.6	10.6	-0.0073	0.01548

III. EXPERIMENTAL RESULTS

The particular attention in this work was paid to bubble behavior. However, to identify PNVG condition status of void content in the heated channel was considered firstly.

A. Void Evolution and Measurement Method

It is known that in heated channel void existence commenced with appearance of first bubble at the location of ONB. In according to last study of present authors, bubble behavior at the incipient of boiling was categorized into sliding and lift-off bubbles [10]. In this study, it was observed that bubbles after nucleation left its origin and slid nearby heated surface. Fig. 2 depicted the typical bubble behavior at incipient of boiling. It was also observed that along bubbles motion some of them survived and moved to downstream and some of them collapsed and vanished in the bulk liquid. In Fig. 3, example of snapshots that depicted bubbles size and their scattering in the heated channel was shown in different liquid subcooling of Exp. I. Because of bubble motion the optical void probe can sense bubbles even at ONB; therefore the lateral distributions of void fraction were measured using the optical void probe in all runs of this experimental study.

Void profiles for two sets of experimental condition are depicted in Fig. 4a and b, respectively. Here, y denotes the distance from the heated surface. It can be seen that the peak of the void fraction and the bubble layer thickness increased with an increase of inlet liquid temperature.

To find out the condition of the onset of net vapor generation, the time-average cross-sectional void fraction <α> was determined by (1):

$$<\alpha>=\left(l_h/A_0\right)\int_0^{w_0}\alpha_{lta}\,dy \qquad (1)$$

where α_{lta} is the local time-averaged void fraction and A_0, w_0 and l_h are cross-sectional area (200 mm^2), the lateral channel width (10 mm) and the width of heated surface (10 mm).

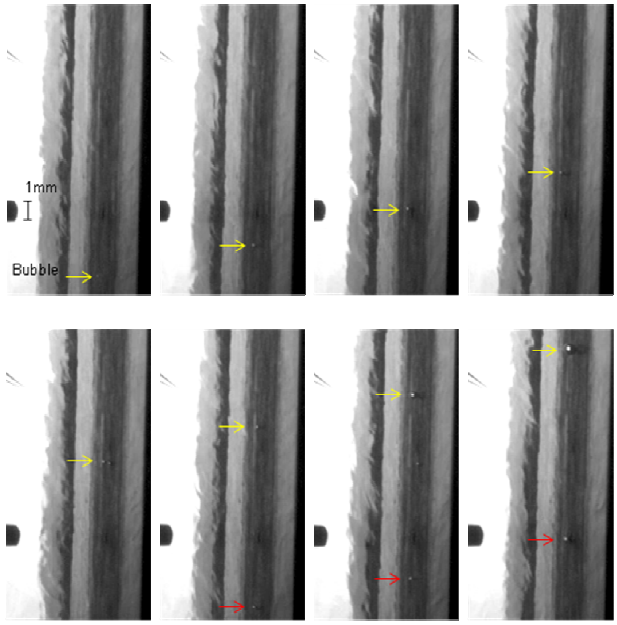

Fig. 2 Typical bubble behavior observed in Exp. I at the ONB (time interval = 0.01s)

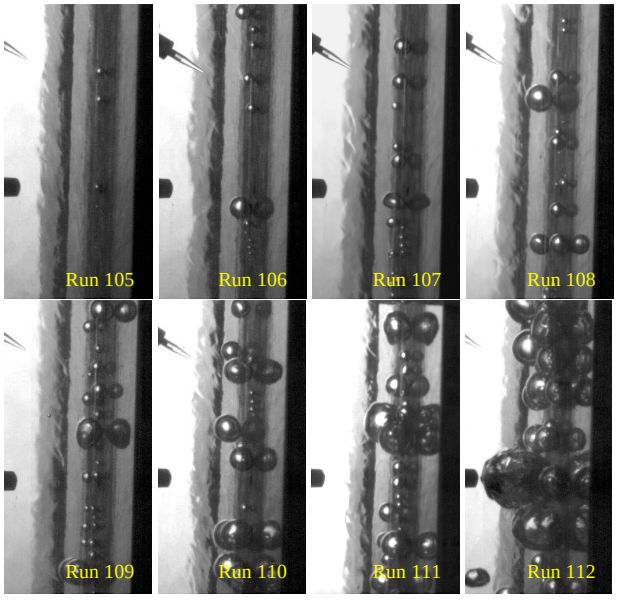

Fig. 3 Examples of snapshot illustrate void status for Exp. I

The values of <α> are plotted against the thermal-equilibrium quality x_{eq} in Fig. 5a and b, respectively; here, axial thermal quality and liquid subcooling are related by following equation:

$$x_{eq}(z) = 1/h_{fg}\left[\left(q_w l_h / GA_0\right) z - c_{pl}\Delta T_{sub}\right] \quad (2)$$

where h_{fg} is the latent heat of vaporization.

In accordance with Fig. 5, the evolution of the vapor void fraction in the subcooled boiling region can be divided into the two regions. In the high liquid subcooling region, sufficiently high wall superheat permits the formation of bubbles at the nucleation cavities commence from ONB, but the void fraction

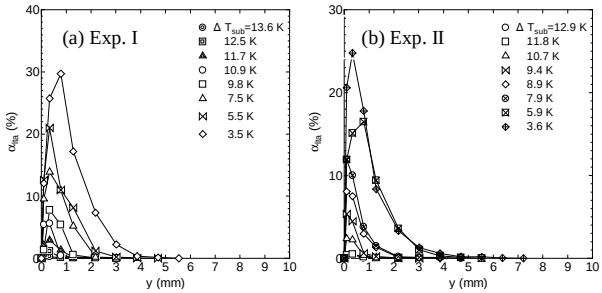

Fig. 4 Dependence of the lateral void fraction distribution to the liquid subcooling for two sets of experiment

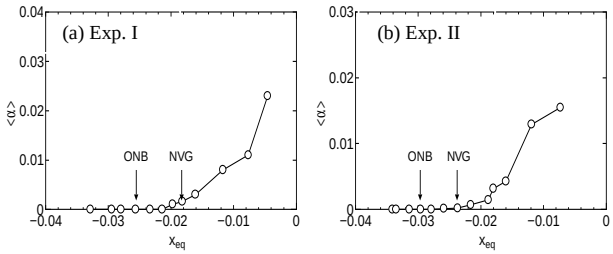

Fig. 5 Dependence of the time-average cross-sectional void fraction on x_{eq} for two sets of experiment

Only in the downstream region of low liquid subcooling, a rapid increase of the vapor void fraction with an increase of x_{eq} was observed. The boundary between two regions, PNVG, was determined in Fig. 5 as well as specified in the Tables I and II.

It was mentioned [3] that the best practical and the simplest correlation for the NVG was postulated by Saha and Zuber [5]. Comparison of $\Delta T_{sub,NVG}$ with Saha and Zuber correlation have resulted a good consistency and the differences are just between 1 to 2 K.

IV. Discussion

In the present work, it was seen that bubbles left the active nucleation site and moved in proximity of heated surface in all the experimental conditions and in various void fractions. Therefore, the well known triggering mechanism of the NVG (i.e. the bubble departure from the nucleation site or the bubble lift-off from the heated surface) is likely to be doubtable, at least for this study. Here, development of void fraction in subcooled boiling was investigated through analyzing vaporization and condensation rate with particular attention to bubble dynamics. The continuity equation of the vapor phase in the steady state condition is given by

$$d(\alpha\rho_g u_g)/dz = \Gamma_V - \Gamma_C = \Gamma_{Net} \quad (3)$$

where z is the axial coordinate, ρ is the density, u is the velocity in the vertical direction, Γ_V is the vaporization rate, Γ_C is the

condensation rate, Γ_{Net} is the net vaporization, and the subscript g denotes the vapor phase. If ρ_g and u_g are assumed to be

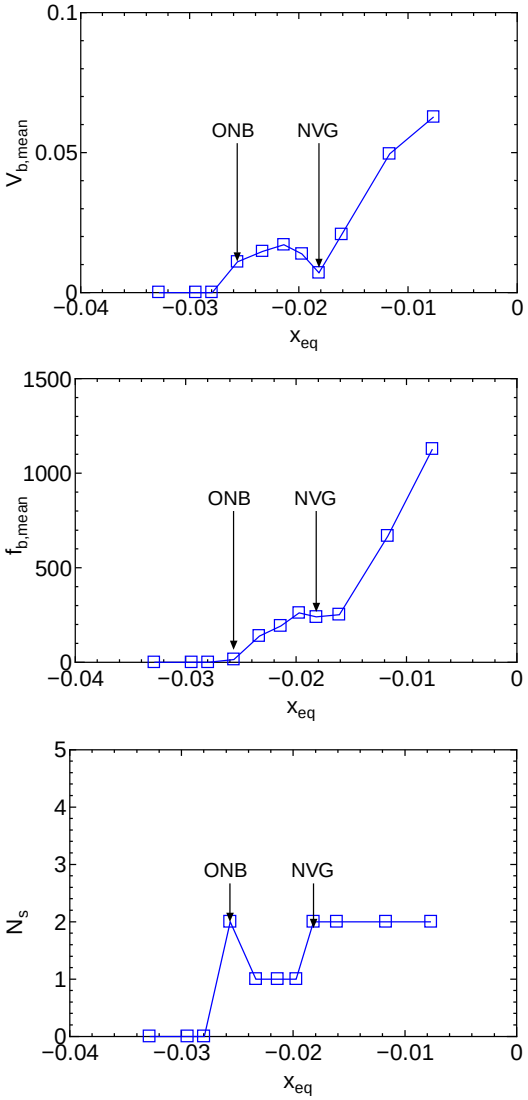

Fig. 6 Variation status of $V_{b,mean}$, $f_{b,mean}$ and N_s in Exp. I

constant for simplicity, (3) combined with (2) can be simplified to (4):

$$d\alpha/dx_{eq} = \left(GAh_{fg}/q_w W_h \rho_g u_g\right)(\Gamma_V - \Gamma_C) \tag{4}$$

Refer to (4) the difference between Γ_V and Γ_C is of importance for α to increase with an increase in x_{eq}. Observation window was considered as a control volume and Γ_V and Γ_C was measured using image analysis. In order to obtain amount of vaporization and condensation rate, bubble characteristics was measured case by case. The vaporization rate Γ_V could simply be calculated using following equation

$$\Gamma_V = \rho_g V_{b,mean} f_{b,mean} N_s / V_{win} \tag{5}$$

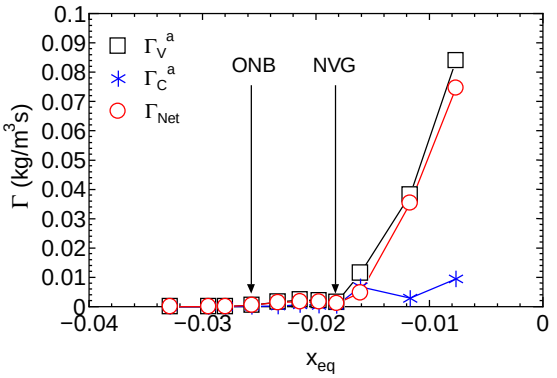

Fig. 7 Vaporization, condensation and net vaporization rate in observation window for Exp. I

where $V_{b,mean}$, $f_{b,mean}$, N_s and V_{win} are mean bubble volume which nucleated within observation window, mean release frequency of bubbles, active nucleation sites in observation window and volume of the channel corresponding to observation window, respectively.

The vaporization process of all the experiments was recorded using high speed camera. The view direction of recoding was chosen as similar as illustrated in Fig. 2. This view direction provides wide enough span of heated surface to investigate bubble characteristics. However, when the inlet temperature is close to saturation temperature huge number of bubbles appears in the channel and therefore bubble overlapping obstructs perfect observation and hence affects image analysis. Furthermore, since measurement of bubble characteristics in low pressure is more accurate and more available, here only the Exp. I was considered. In this condition all the active nucleation sites N_s can be counted from ONB condition to several runs after PNVG. In addition, with concentration on all the active nucleation sites and counting bubble ebullition within a certain time the mean release frequency of bubble $f_{b,mean}$ was measured. To obtain mean bubble volume $V_{b,mean}$ all the nucleate bubbles in the observation window were followed one by one. It is evident that vaporization process will be completed when nucleate bubble achieve to maximum size in its motion; and afterward however it may be collapsed or survived. In case of collapsing, condensation rate was measured separately. For two sets of experiment $V_{b,mean}$, $f_{b,mean}$ and N_s were measured and shown in Fig. 6.

The condensation rate Γ_C was measured simply by

$$\Gamma_C = \left(\rho_g / V_{win} t_0\right) \sum_{i=0}^{N_C} V_{b,mean} \tag{6}$$

where N_C is the number of bubbles that are collapsed in the observation window during t_0.

In Fig. 7 the value of Γ_V, Γ_C and Γ_{Net} are plotted against x_{eq}. It is seen that Γ_V and Γ_C take positive value after ONB but because they are small and almost similar, Γ_{Net} is close to zero. However, one run after PNVG Γ_V is greater than Γ_C and hence

net evaporation rate Γ_{Net} rise up, sharply. Therefore, this figure confirmed the expectation regard with (4): in proximity of PNVG where gradient of α was changed significantly, Γ_{Net} also increased sharply. Furthermore, it is seen that Γ_V also has a significant change after PNVG as similar as Γ_{Net}; in contrast, Γ_C was not affected so much. It can be hence to say that in presence of low condensation, void is mostly influenced by vaporization rate after PNVG.

In order to understand mechanism of causing significant increment of void fraction or net vaporization rate, the bubble behavior and its characteristics were recognized with more detail. According to (5) it can be concluded that Γ_V is corresponding to two factors: the first is mean bubble volume $V_{b,mean}$ and the other is population of nucleate bubble or total bubble generation ($N_s f_{b,mean}$). In accordance with $V_{b,mean}$, Fig. 6 illustrated that $V_{b,mean}$ was enhanced obviously after PNVG. Therefore, this factor contribute void to increase sharply after PNVG. On the other hand, it is seen that $f_{b,mean}$ was increased significantly, but N_s were changed between 1 and 2 numbers. With value of N_s and $f_{b,mean}$ total bubble generation in the observation window was obtained and was shown in Fig. 8. In this figure total bubble generation also increase significantly after PNVG. Therefore, not only $V_{b,mean}$ is an influential parameter to rise up vaporization rate after PNVG, but also increase of total bubble generation is another effective factor.

Here, bubble generation before and after PNVG was investigated with more detail to find reasons causing increase of bubble size and bubble population. Concentrate on

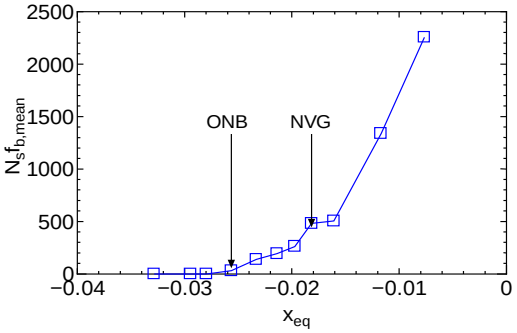

Fig. 8 Total bubble generation in observation window in Exp. I

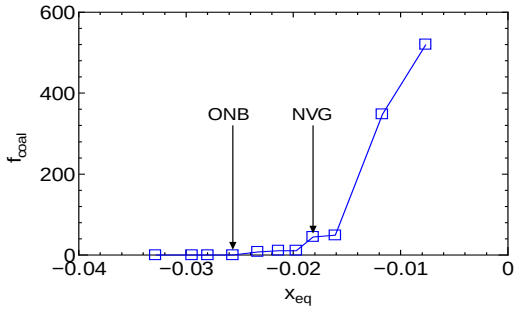

Fig. 9 Bubble coalescence frequency in proximity of nucleation site in several runs of Exp. I

Sites revealed that bubbles before PNVG were created very sporadic. It is seen that at a moment some bubbles nucleate on the surface and then cease for a while. These bubbles left nucleation site and moved along heated surface and after short sliding were mostly vanished in the subcooled liquid. In contrast, after PNVG bubble generation is likely to be consecutive and ceaseless. Therefore, it was seen that bubble release frequency was significantly increased as was seen in Fig. 6. Moreover, with the increase of bubble frequency waiting time of bubble ebullition was decreased. Hence, it is expected that with the consistent bubble creation coalescence of bubbles occur frequently at the instant of creation.

For a nucleation site which is activated from ONB and maintained active in all runs of experiment, bubble coalescence frequency f_{coal} was measured. The result is shown in Fig. 9. It is seen that f_{coal} sharply rise up after PNVG. This figure shows that bubble coalescence takes place frequently among nucleate bubbles mostly after PNVG. Typical bubble coalescence in proximity of the nucleation site is shown in Fig. 10 for Run 110. In this Figure, instance of bubble coalescence was remarked with a circle. It is evident that the result of coalescence is augmentation of bubble volume. It was expressed and also was observed in this study that the increase in bubble size decreases interfacial area concentration, in a given void fraction, causing suppression of condensation rate. [14]. Therefore, it can be concluded that rise up of bubble population is associated with increment of bubble coalescence which leads to more bubble survival. In consequence, it was observed that coalesced bubbles when are little distanced from nucleation site, slide beside heated surface and grow up, significantly. Therefore, after PNVG mean bubble volume not only because of coalescence is augmented, but also it significantly increases due to sliding beside heated surface.

V. Summarizes and Conclusion

Vapor bubble behavior and its characteristics were investigated in an upward rectangular channel under subcooled flow boiling regimes. The heated surface was hydrophilic and experiments were performed under moderate pressure. Inlet temperature was chosen as a variable parameter though to change x_{eq} parametrically. Under high subcooling conditions, when boiling was commenced at ONB, bubbles departed the active nucleation site immediately after nucleation and slid along heated channel in proximity of heated surface. Therefore, it was concluded that bubble departure in not triggering mechanism of NVG, at lease for this experimental condition. From ONB to slightly downstream region it was observed that in course of bubble motion some of them were collapsed and some of them survived in the subcooled liquid. Since the vaporization rate was not significant and condensation rate was nearly equal to the vaporization rate, an increase in the vapor void fraction with an increase in the x_{eq} was small. On sufficiently high inlet temperature, the bubble population and the bubble volume were increased sharply. It was found that these two parameters contributed to increase significantly of void fraction after PNVG.

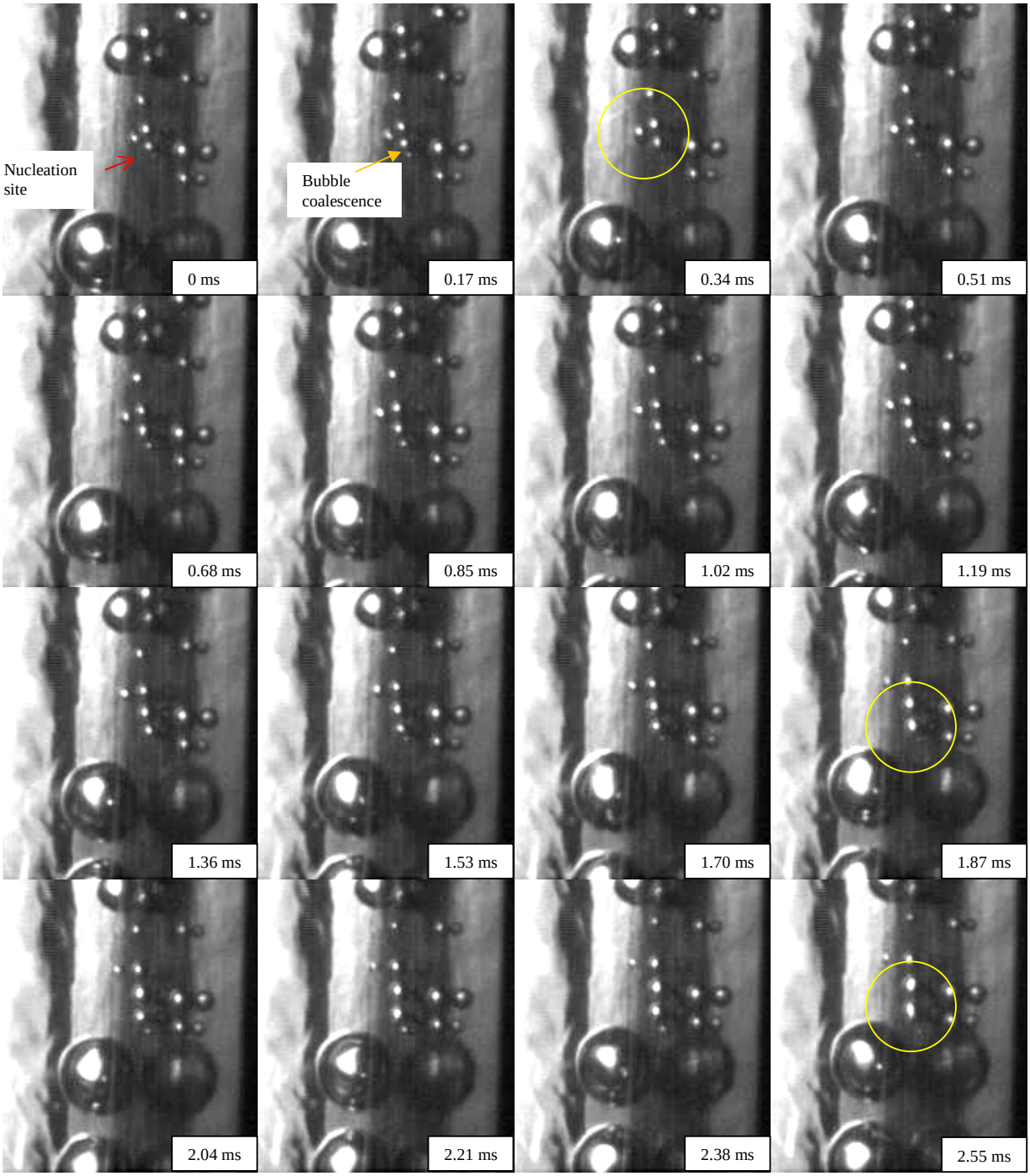

Fig. 10 Example of bubble coalescence for Exp. I, Run 110

Detail observation showed that with the increase of release frequency of bubbles waiting time of bubble nucleation was decreased, considerably. Consequently, it was found that bubble coalescence frequency at the instant of nucleation was increase sharply, after PNVG. The result of coalescence is augmentation of bubble and depression of condensation rate. In the other words, it can be concluded that by bubble coalescence population of bubbles that can be survived in the channel is increased. On the other hand, it was observed that in this condition bubble life time is long enough to slide on heated surface and grow up, significantly. Therefore, increase of void fraction after PNVG, can be attributed to significant increment of bubble population and also mean bubble volume.

ACKNOWLEDGMENT

This work was supported by KAKENHI (No. 20360419).

REFERENCES

[1] S. C. Lee and S. G. Bankoff, Prediction of the onset of flow instability in transient subcooled flow boiling, Nuclear Engineering and Design, Vol. 139, 1993, pp. 149-159
[2] P. G. Kroeger, N. Zuber, An analysis of the effects of various parameters on the average void fractions in subcooled boiling, International Journal of Heat and Mass Transfer, Vol. 11, 1968, pp. 211–233.
[3] S. C. Lee and S. G. Bankoff, A Comparison of Predictive Models for the Onset of Significant Void at Low Pressures in Forced-Convection Subcooled Boiling, KSME International Journal, Vol. 12, No. 3, 1998, pp. 504-513
[4] S. Levy, Forced convection subcooled boiling prediction of vapor volumetric fraction, International Journal of Heat and Mass Transfer 10, 1967, pp. 951–965.
[5] P. Saha, N. Zuber, Point of net vapor generation and vapor void fraction in subcooled boiling, Proceedings of the 5th Heat Transfer Conference, Tokyo, Japan, 1974, pp. 175–179.
[6] Bowring, R. W., 1962, Physical Model Based on Bubble Detachment and Calculation of Steam Voidage in the Subcooled Region of a Heated Channel, HPR-10, Institutt for Atomenergi, Halden, Norway.
[7] J.T. Rogers, M. Salcudean, Z. Abdullah, D. McLeod, D. Poirier, The onset of significant void in up-flow boiling of water at low pressure and velocities, International Journal of Heat and Mass Transfer 30, 1987, pp. 2247–2260.
[8] J.G. Collier, J.R. Thome, Convective Boiling and Condensation, third ed., Oxford University Press, Oxford, 1994. pp. 325–374.
[9] G. R. Warrier & V. K. Dhir , Heat Transfer and Wall Heat Flux Partitioning During Subcooled Flow Nucleate Boiling—A Review, Journal of Heat Transfer 128, 2006, pp. 1243–1256.
[10] R. Ahmadi, T. Ueno, T. Okawa, Bubble dynamics at boiling incipience in subcooled upward flow boiling, International Journal of Heat and Mass Transfer 55 (1-3), 2012, pp. 488-497.
[11] Dix, G. E., Vapor Void Fraction For Forced Convection with Subcooled Boiling at Low Flow Rates, 1971, Ph.D. thesis, University of California, Berkeley.
[12] E.L. Bibeau, M. Salcudean, A study of bubble ebullition in forced-convective subcooled nucleate boiling at low pressures, International Journal of Heat and Mass Transfer 37, 1994, pp. 2245–2259.
[13] T. Okawa, T. Ishida, I. Kataoka, M. Mori, Bubble rise characteristics after the departure from a nucleation site in vertical upflow boiling of subcooled water, Nuclear Engineering and Design 235, 2005, pp. 1149–1161.
[14] O. Zeitoun, M. Shoukri, Bubble behavior and mean diameter in subcooled flow boiling, Transactions of ASME, Journal of Heat Transfer 118, 1996, pp. 110–116

Rouhollah Ahmadi: This author is a PhD Candidate in Mechanical engineering at Osaka University, Japan. He was born in Iran at 1980. He got MSc. degree of Mechanical Engineering in field of thermal and fluid mechanics from Sharif University of technology, Tehran, Iran in 2007. He published three journal papers in the field of thermal-fluid mechanics, and also has several papers that are presented in valid conferences. Furthermore, he has 5 years experience as quality control manager in two manufacturing companies in field of constructing of heating and cooling equipments as well as pressure vessels.